Pigmented Paravenous Chorioretinal Atrophy: Clinical Spectrum and Multimodal Imaging Characteristics

EUN KYOUNG LEE, SANG-YOON LEE, BAEK-LOK OH, CHANG KI YOON, UN CHUL PARK, AND HYEONG GON YU

• PURPOSE: To investigate the clinical findings and natural course of patients with pigmented paravenous chorioretinal atrophy (PPCRA) using multimodal imaging.
• DESIGN: Retrospective, observational case series.
• METHODS: We reviewed the records of consecutive patients diagnosed with PPCRA at a single center and assessed serial fundus photographs, fundus autofluorescence (FAF), and spectral-domain optical coherence tomography images. Electrophysiological findings and visual field analysis were also reviewed.
• RESULTS: The study included 50 eyes in 25 patients. The mean age of the population was 51.6 ± 14.6 years. Nine patients (36.0%) were asymptomatic and 9 (36.0%) complained of nyctalopia. We divided fundus appearance into one of 3 groups: paravenous (58.0%), focal (16.0%), and confluent (26.0%). Of the 50 eyes, macular involvement was present in 13 eyes (26.0%). Fifteen patients (60.0%) demonstrated a symmetric fundus appearance, whereas 10 (40.0%) had marked asymmetry. Eight eyes (16.0%) exhibited apparent changes in fundus findings, over a mean follow-up period of 8.8 years. FAF imaging was most sensitive to evaluate the extent of lesions. Sixteen eyes (44.4%) showed progressive visual field loss during the follow-up period. Most patients maintained stable vision, and 36 eyes (72.0%) had a final visual acuity of 20/50 or better. Nevertheless, some eyes with macular involvement experienced severe deterioration in vision. Electrophysiological data were variable, and interocular asymmetry was common (45.8%).
• CONCLUSIONS: PPCRA can present with a more variable expressivity than previously described. Multimodal imaging can provide insights into its clinical characteristics to facilitate the diagnosis, classification, and follow-up of these patients. (Am J Ophthalmol 2021;224:120–132. © 2020 Elsevier Inc. All rights reserved.)

AJO.com Supplemental Material available at AJO.com.
Accepted for publication Dec 7, 2020.

From the Department of Ophthalmology, Seoul National University College of Medicine, Seoul National University Hospital (E.K.L., B.L.O., C.K.Y., U.C.P., H.G.Y.), Seoul, Republic of Korea; and SNU Blue Eye Clinic (S.Y.L.), Seoul, Republic of Korea.

Inquiries to Hyeong Gon Yu, Department of Ophthalmology, Seoul National University College of Medicine, Seoul National University Hospital, #101, Daehak-ro, Jongno-gu, Seoul 03080, Republic of Korea; e-mail: hgonyu@snu.ac.kr

PIGMENTED PARAVENOUS CHORIORETINAL ATROPHY (PPCRA) is a rare form of chorioretinal atrophy characterized by perivenous aggregations of pigment clumps associated with peripapillary and radial zones of retinal pigment epithelial atrophy that are distributed along the retinal veins.[1] It was first referred to as retinochoroiditis radiata in 1937.[2] Since then, a few case reports and small series have been published.[3–6] It has been commonly reported to be bilateral and symmetric. Patients are usually asymptomatic, and the diagnosis is primarily based on its characteristic appearance on fundus examination.

The cause of the condition is unknown, and genetic, inflammatory, and infectious causes have been suggested. Most cases are reported to develop sporadically, but there are specific cases of familial occurrence.[7–12] One study reported a heterozygous *CRB1* mutation identified in a family with dominantly inherited PPCRA with variable expressivity.[11] Therefore, there has been varied speculation about the mode of inheritance; however, there remains no convincing evidence. Meanwhile, inflammatory/infectious etiologies have been hypothesized. Early studies described cases of PPCRA that developed after an inflammatory disease, including Behçet disease,[13] measles,[14] rubeola,[15] congenital syphilis,[16] and uveitis.[17] However, the recent literature is in consensus that these changes are related to retinal vein vasculopathy resulting from various inflammatory causes and should be considered as pseudo-PPCRA.[18]

Although a clinical diagnosis of PPCRA is made based on a typical fundus appearance, detailed multimodal retinal imaging and electrophysiology are helpful in confirming the diagnosis. Given that the number of reported case series is very limited, a better understanding of this rare disease requires more information. This study aimed to examine the clinical presentation across a broad spectrum of PPCRA in 25 patients using detailed multimodal imaging. Furthermore, we aimed to elucidate the natural course and pathogenesis of the disease based on long-term follow-up observations.

METHODS

• PARTICIPANTS AND CLINICAL ASSESSMENT: This study was performed at the Seoul National University Hospital in

0002-9394/$36.00
https://doi.org/10.1016/j.ajo.2020.12.010

Korea. The study followed the tenets of the Declaration of Helsinki and was approved by the Institutional Review Board at Seoul National University Hospital (IRB approval number: 2004-172-1119). We retrospectively reviewed the medical records of patients diagnosed with PPCRA between 2002 and 2019. The diagnosis of PPCRA was made by a physician based on the following criteria: typical and characteristic fundus appearance of chorioretinal atrophy with bone corpuscular pigmentation along the retinal veins in one or both eyes, corresponding visual field defect, and electroretinography (ERG) findings. Patients with retinitis pigmentosa (RP) were excluded from the study. The diagnosis of RP was based on the following criteria: history of night blindness, bone spicule pigmentary retinopathy, nonrecordable ERG, and typical visual field defect by perimetry. The clinical data included age, sex, ethnicity, presence of symptoms, family history of inherited retinal disease, and previous ocular inflammation/infection.

• **OCULAR EXAMINATION:** All patients underwent comprehensive ophthalmic examinations, including measurement of best-corrected visual acuity (BCVA), slit-lamp biomicroscopy, and indirect fundus examination. Fundus photography and fluorescein angiography (FA) were obtained using either a fundus camera (Vx-10; Kowa OptiMed, Tokyo, Japan) or ultrawide-field fundus photography (Optos 200Tx; Optos PLC, Scotland, UK). We obtained spectral domain optical coherence tomography (SD-OCT) images using either a Heidelberg Spectralis (Heidelberg Engineering, Heidelberg, Germany) or Zeiss Cirrus (Cirrus 4000; Carl Zeiss Meditec, Dublin, California, USA). Fundus autofluorescence (FAF) images were obtained using either a Spectralis HRA (Heidelberg Engineering) or Optos widefield camera. We performed visual field examination using either a Humphrey Field Analyzer (Humphrey visual field Analyzer II with Swedish Interactive Threshold Algorithm standard 24-2 or 30-2; Carl Zeiss Meditec) or a Goldmann manual perimeter (Haag–Streit, Berne, Switzerland). Full-field ERG were performed using gold foil recording electrodes and incorporated the ISCEV (International Society for Clinical Electrophysiology of Vision) standard protocols.[19] In selected patients, we also performed indocyanine green angiography (ICG, Heidelberg Engineering) and swept-source optical coherence tomography angiography (OCTA, PLEX Elite 9000; Carl Zeiss Meditec). The BCVA measurements were converted to logarithm of minimal angle of resolution (logMAR) units before analysis.

RESULTS

• **DEMOGRAPHICS:** The study included 50 eyes from 25 patients with a diagnosis of PPCRA. The Table summarizes the patient demographics and clinical characteristics. The mean age of the subjects was 51.64 ± 14.58 years (range 29-82 years). Eleven patients (44.0%) were male and 14 (56.0%) were female. All patients were Asian (Korean). None of the patients reported a family history of inherited retinal disease except that 2 patients reported having a mother with poor night vision. Most study participants were generally healthy. Pre-existing conditions included hypertension, hypothyroidism (1 patient); diabetes, hypertension (2 patients); hypertension (1 patient); thymoma (1 patient); and chronic obstructive pulmonary disease (COPD) (1 patient). Four patients taking antihypertensive and/or diabetes medications due to pre-existing conditions and 1 patient diagnosed with COPD taking bronchodilators were included. However, none of the patients were diagnosed with rheumatic disorders or had a history of taking hydroxychloroquine in this study cohort. Moreover, although retinal antibodies could not be investigated in the included patients, none of the

TABLE. Demographic and Clinical Characteristics of Patients With Pigmented Paravenous Chorioretinal Atrophy (No. of Eyes = 50)

Variable	Eyes With PPCRA
Age, y	51.64 ± 14.58
Male/female	11/14
PPCRA phenotype	
Paravenous	29 (58.0)
Focal	8 (16.0)
Confluent	13 (26.0)
Macular involvement	13 (26.0)
Symmetricity of fundus appearance	
Symmetric	15 (60.0)
Asymmetric	10 (40.0)
FAF hyperAF ring	12 (24.0)
Visual field defect	
Peripheral constriction	2 (4.2)
Enlarged blind spot	6 (12.5)
Geographic scotoma	27 (56.3)
Central and temporal islands	4 (8.3)
Central island	7 (14.6)
Peripheral islands	1 (2.1)
VA at baseline (logMAR)	
Right eye	0.34 ± 0.83
Left eye	0.43 ± 0.81
VA at final visit (logMAR)	
Right eye	0.54 ± 1.02
Left eye	0.60 ± 0.92
Symmetricity of ERG	
Symmetric	13 (54.2)
Asymmetric	11 (45.8)

ERG = electroretinography, FAF = fundus autofluorescence, hyperAF = hyperautofluorescent, logMAR = logarithm of minimal angle of resolution, PPCRA = pigmented paravenous chorioretinal atrophy, VA = visual acuity.

Continuous variables are reported as mean value ± standard deviation. All other data are numbers (percentages).

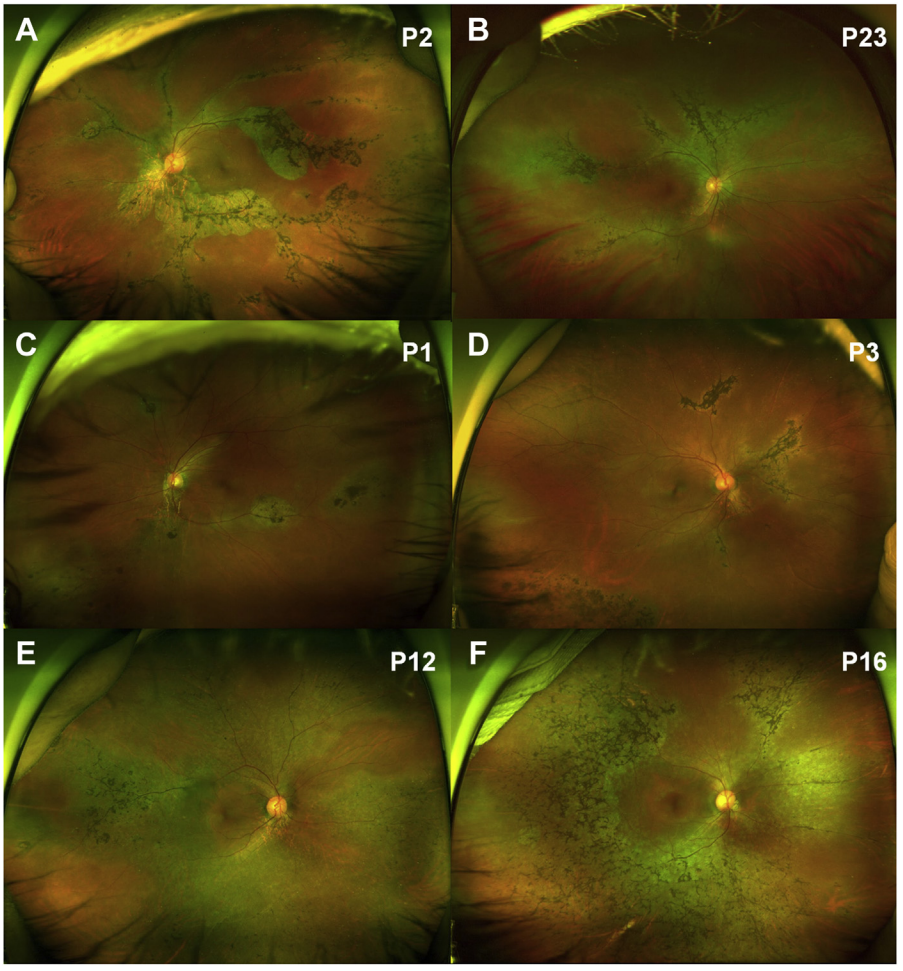

FIGURE 1. Ultrawide-field fundus photography of patients with various phenotypes of PPCRA: (A, B) Paravenous type, (C, D) focal type, (E, F) confluent type. P = patient number, PPCRA = pigmented paravenous chorioretinal atrophy.

patients had a history of malignancy or autoimmune disease, except for one who had undergone surgery 20 years ago due to benign thymoma. Therefore, the diagnosis of hydroxychloroquine retinopathy or autoimmune retinopathy, which may exhibit findings similar to those of PPCRA, could be excluded. In these patients, we also found no evidence of active or previous ocular inflammation or infection. Of the 25 patients, 9 (36.0%) were asymptomatic and were found incidentally during routine examination. Two (8.0%) patients were referred after a regular checkup but complained of a history of night blindness. In patients who were symptomatic, the presenting symptoms included a deterioration of visual acuity (8 patients, 32.0%), nyctalopia (7 patients, 28.0%), and peripheral visual field reduction (2 patients, 8.0%). All patients had bilateral disease but it appeared to have variable expressivity. The mean follow-up period was 5.74 years (range 0-17.5 years), with 1 patient only attending a single visit.

• **CLINICAL FINDINGS—FUNDUS APPEARANCES:** Supplementary Table S1 demonstrates the fundus and FAF findings. Refraction data were available in 16 of 25 patients. The mean spherical equivalent refraction was –0.23 ± 1.96 diopters (D) (range –4.63 to +3.75 D). All patients demonstrated chorioretinal atrophy that was distributed along the retinal veins but showed differences in the extent of the fundus that was involved and the presence of pigmentary disturbances. We classified eyes into one of 3 groups according to the fundus appearance: (1) the "paravenous" type was characterized by typical chorioretinal atrophy with pigment clumping continuously connected in a geographic manner (Figure 1, A and B); (2) the "focal" type was characterized by localized chorioretinal atrophy with pigment clumping that are separated with each other (Figure 1, C and D); (3) the "confluent" type was characterized by chorioretinal atrophy with bone spicules that are extensively combined with each other and often mistaken for RP (Figure 1, E and F). Among the 50 eyes, the paravenous type was the most common and was present in 29 eyes (58.0%). The focal type was present in 8 eyes (16.0%) and the confluent type was present in 13 eyes (26.0%), constituting the second-most common types.

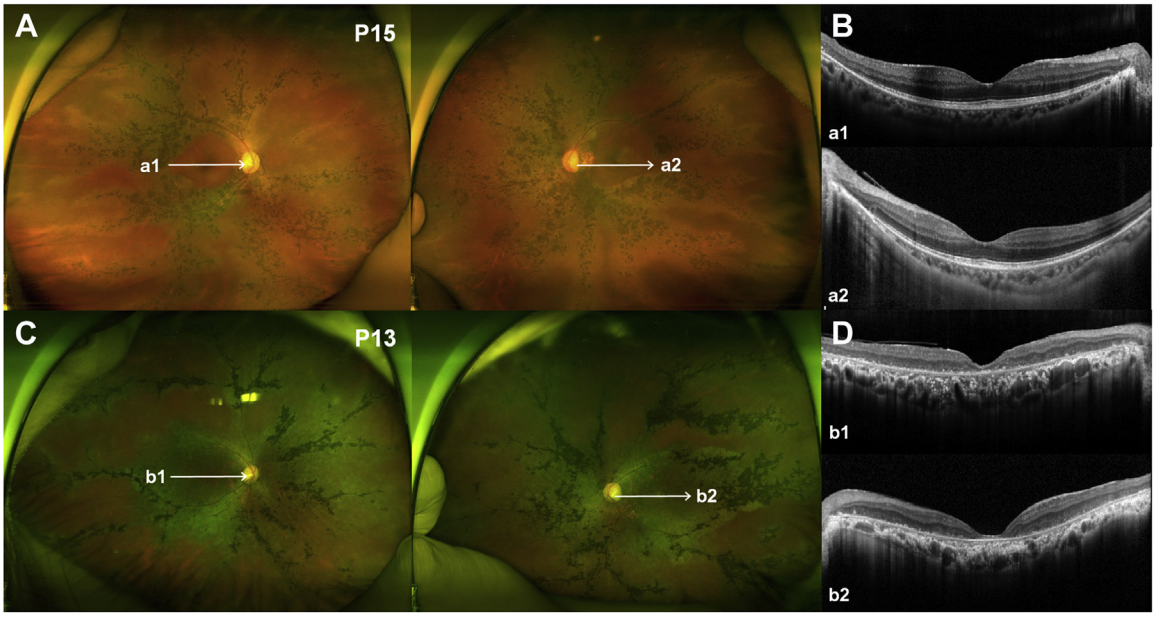

FIGURE 2. Ultrawide-field fundus photography and OCT scans of a patient (A, B) without macular involvement and (C, D) with macular involvement. A, B. The horizontal OCT scans at the corresponding areas on A (white arrows, a1 and a2) reveal a normal foveal contour and intact photoreceptor and retinal pigment epithelial morphology. C, D. The horizontal OCT scans at the corresponding areas on C (white arrows, b1 and b2) demonstrate a severely disrupted outer retina, foveal microstructure, and retinal pigment epithelium. OCT = optical coherence tomography, P = patient number.

• **CLINICAL FINDINGS—MACULAR INVOLVEMENT:** Macular involvement was defined as chorioretinal atrophy involving the fovea. Of the 50 eyes, the macula was spared in 37 eyes (74.0%) (Figure 2, A and B) and macular involvement was observed in 13 eyes (26.0%) (Figure 2, C and D). The severity of pigmentary disturbance varied among those with macular involvement. Macular optical coherence tomography (OCT) images in eyes with macular involvement exhibited severe disruption of the outer retina and retinal pigment epithelium (Figure 2, D). Of the 13 eyes with macular involvement, the ellipsoid zone (EZ) band, interdigitation zone (IZ) band, and retinal pigment epithelial line were lost on the macular OCT images in 7 eyes (53.8%); the EZ and IZ bands were lost but the foveal retinal pigment epithelial line was preserved in 2 eyes (15.4%); and the IZ line was lost but the foveal EZ and retinal pigment epithelial lines were preserved in 4 eyes (30.8%). Among the 37 eyes without macular involvement, other macular comorbidities were observed in 3 eyes: a fine epiretinal membrane in 2 eyes and epiretinal membrane with foveoschisis in 1 eye.

• **CLINICAL FINDINGS—SYMMETRY AND PROGRESSION:** In 15 (60.0%) patients, both eyes demonstrated a symmetric fundus appearance (Figure 3, A through D), whereas 10 (40.0%) patients had marked asymmetry (Figure 3, E through H). In patients with asymmetric fundus appearance, the right eye showed more severe involvement than the left eye in 4 (40.0%) patients and the left eye showed more severe involvement than the right eye in 6 (60.0%) patients. Forty-two eyes (84.0%) in 21 patients revealed no obvious changes in fundus photography between the first and final visits, with a mean follow-up period of 5.2 years (range 0-17.5 years). There were 8 eyes (16.0%) in 4 patients who exhibited apparent changes in fundus appearance, over a mean follow-up period of 8.8 years (range 5.7-12.0 years) (Figure 4). The areas of chorioretinal atrophy gradually enlarged and the pigment clumping became darker and wider.

• **IMAGING—OPTICAL COHERENCE TOMOGRAPHY AND OPTICAL COHERENCE TOMOGRAPHY ANGIOGRAPHY:** On macular OCT images, disruptions of the EZ, IZ, and retinal pigment epithelial lines and choroidal thinning underlying the atrophic retinal pigment epithelium were noticed. It was also observed that the macular curvature became steeper as the outer retina and choroid became atrophic. Among the 42 eyes with no obvious changes on fundus photography, 4 eyes demonstrated changes in the integrity of intraretinal microstructures between the first and final visit on macular OCT images.

SD-OCT scans of affected paravenous areas were available in this study (Figure 5). The chorioretinal atrophic areas showed visible thinning of the entire outer retina, including the outer nuclear layer, external limiting membrane, EZ, and IZ band. The bone-spicule pigment exhibited intraretinal hyperreflective plaques across the outer retina or even the entire retina. These nodular

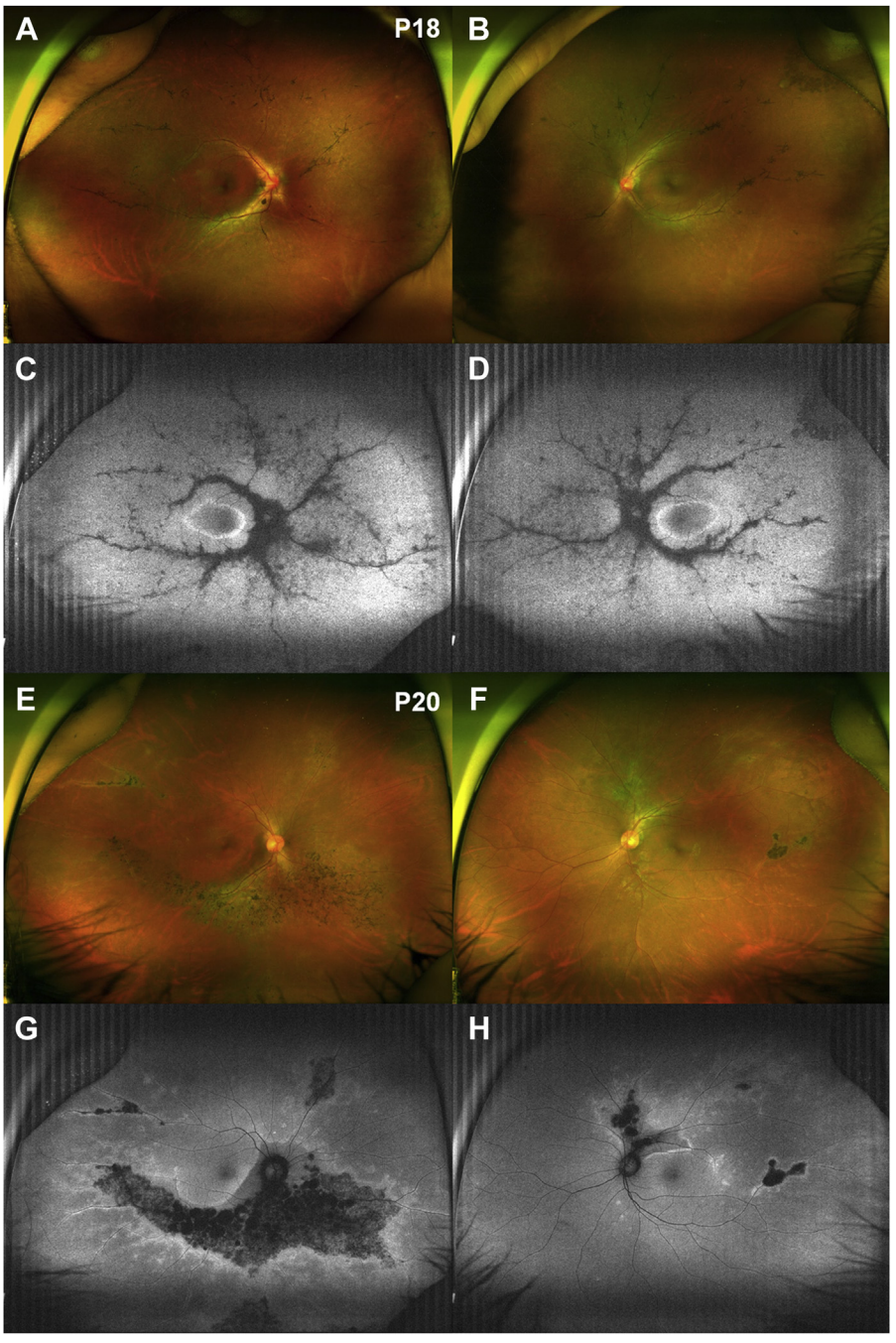

FIGURE 3. Ultrawide-field fundus photography and FAF imaging of patients with (A-D) symmetric fundus appearance and (E-H) asymmetric fundus appearance. A-D. The FAF images of both eyes in patient 18 show a well-demarcated contiguous areas of hypoautofluorescence corresponding to the areas of chorioretinal atrophy. Bilateral ring-shaped hyperautofluorescence were also noted. E-H. The FAF images of both eyes in patient 20 reveal hypoautofluorescence patches with a hyperautofluorescent border. The right eye showed more severe involvement than the left eye. FAF = fundus autofluorescence, P = patient number.

excrescences generate an underlying shadowing on SD-OCT scans.

On SD-OCT images, there were some patients in whom retinal pigment epithelial atrophy was not yet evident within the affected paravenous areas, but the choroidal thickness was clearly reduced compared with that of adjacent areas (Figure 6, A). The choriocapillaris OCTA images demonstrated areas of flow void beneath the retinal pigment epithelial layer, suggestive of choriocapillaris hypoperfusion (Figure 6, B). The relative sparing of the retinal capillary plexuses was observed on OCTA imaging, indicating that the disease primarily affects the choroidal

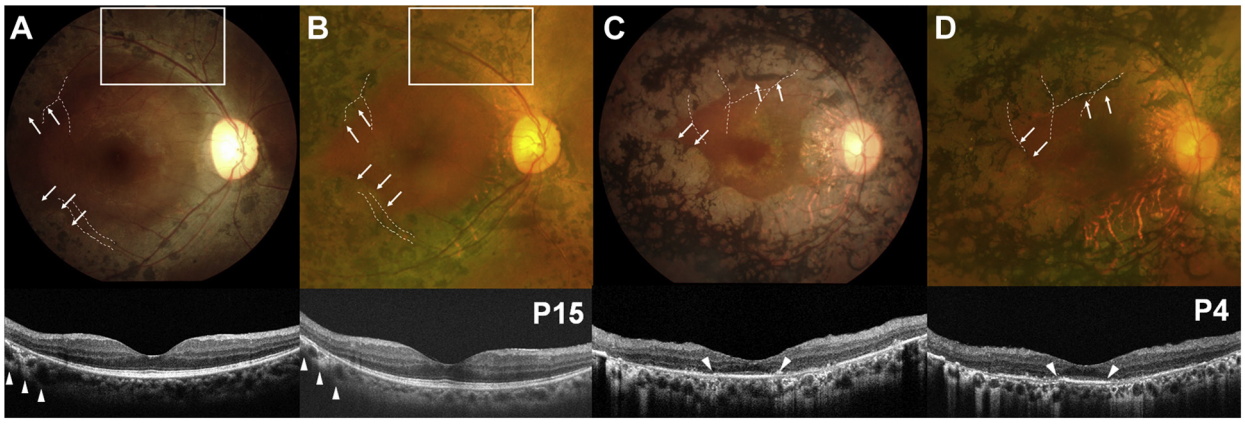

FIGURE 4. Fundus photography and OCT scans of patients with obvious change in fundus appearance. A, B. The chorioretinal atrophic region gradually enlarged (white arrows) compared to the arrangement of retinal vessels (white dotted lines) during the 12-year observation period in patient 15. The pigment clumping also became darker and wider (white boxes). The vertical OCT scans demonstrate visible thinning of the entire outer retina, including the outer nuclear layer, external limiting membrane, ellipsoid zone, and interdigitation zone inferior to the fovea. The retinal pigment epithelium in these areas seems unaffected, but choroidal thickness is clearly reduced (white arrowheads). C, D. The chorioretinal atrophy with perivenous aggregations of pigment clumps (white arrows) were gradually widened, threatening the fovea during the 6-year follow-up in patient 4. The retinal vessels were outlined with white dotted lines. The vertical OCT scans reveal generalized disruption of foveal microstructures with a small area of preserved faint ellipsoid zone and retinal pigment epithelium subfoveally (white arrowheads). OCT = optical coherence tomography, P = patient number.

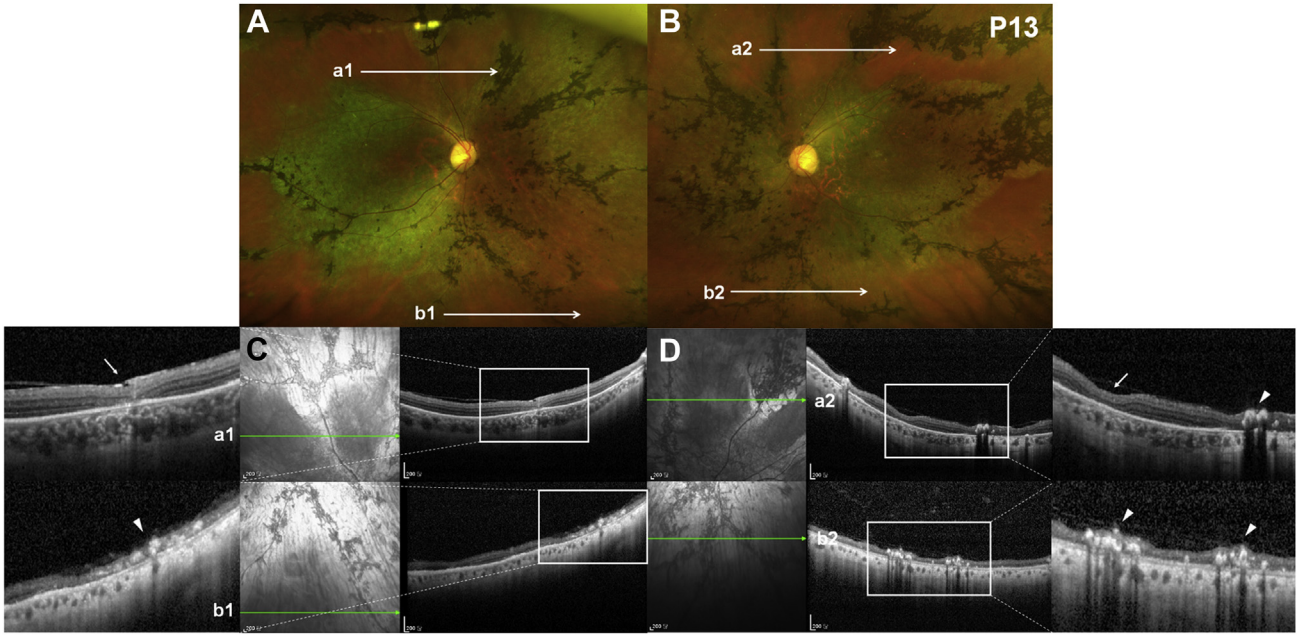

FIGURE 5. (A, B) Fundus photography and (C, D) OCT scans in the affected paravenous areas in patient 13. The horizontal OCT scans are shown to demonstrate the corresponding areas on A and B (long white arrows, a1/b1 and a2/b2). In the region with only chorioretinal atrophy, thinning of the entire outer retina was observed (short white arrows). In the region with chorioretinal atrophy with dark pigment clumping, intraretinal hyperreflective plaques were observed (white arrowheads), which is more remarkable on magnified images (white boxes). These nodular excrescences generate an underlying shadowing in the OCT scans. OCT = optical coherence tomography, P = patient number.

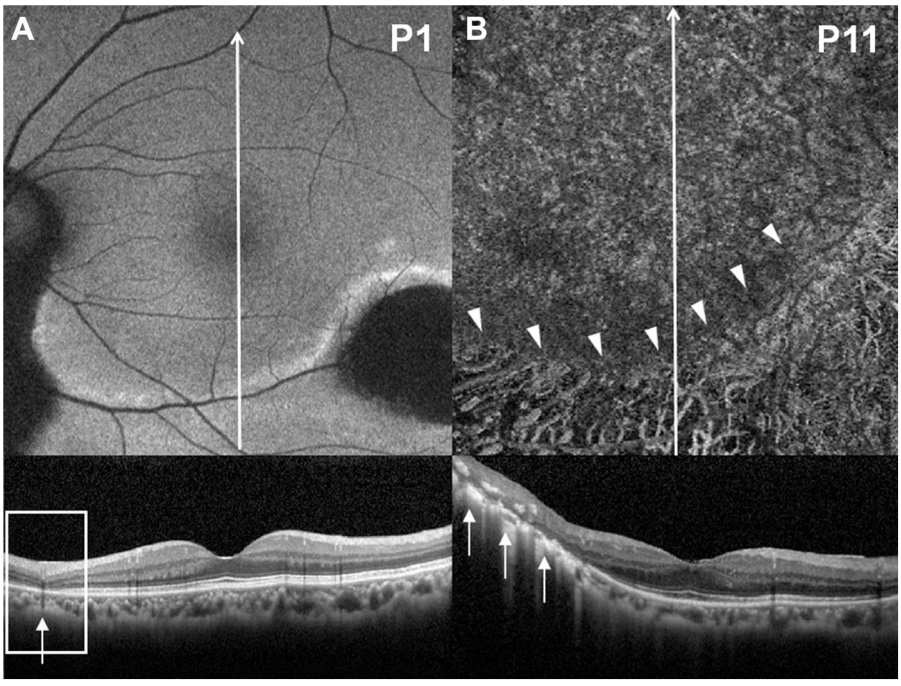

FIGURE 6. The FAF, OCTA, and vertical OCT scans demonstrate the corresponding areas (long white arrows) of patients with PPCRA. A. The OCT image reveals that retinal pigment epithelium atrophy was not yet evident within the affected paravenous areas (white box), but choroidal thickness is decreased compared with that of adjacent areas (short white arrow). B. The OCTA image of the choriocapillaris layer shows areas of flow void beneath the retinal pigment epithelium (white arrowheads). The OCT scan reveals thinning and disorganization of the outer retina and retinal pigment epithelial disruption. Loss of choroidal architecture within the affected paravenous areas are also noted (short white arrows). FAF = fundus autofluorescence, OCT = optical coherence tomography, OCTA = optical coherence tomography angiography, P = patient number, PPCRA = pigmented paravenous chorioretinal atrophy.

vascular network, with a relative sparing of the retinal vasculature.

• **IMAGING—FUNDUS AUTOFLUORESCENCE:** We present a modified classification of the FAF, comprising "paravenous," "focal," and "confluent" in this study, because it was difficult to clearly distinguish Type 1a and 1b, which have previously been described by Shona and associates.[20] Paravenous type was characterized by continuous hypoautofluorescent signal along the large retinal veins in a geographic manner surrounded by linear hyperautofluorescence extending to the periphery (Supplementary Figure S1, A and B). Focal type was characterized by focal hypoautofluorescent signals that were separate from each other (Supplementary Figure S1, C and D). Confluent type was characterized by extensive areas of hypoautofluorescent signal coalescing and extending beyond the vasculature (Supplementary Figure S1, E and F). In good agreement with the previously classified fundus appearance, 29 eyes (58.0%) presented with paravenous, 8 eyes (16.0%) with focal, and 13 eyes (26.0%) with confluent fundus on FAF images. On the FAF images, ring-shaped hyperautofluorescence was observed in 12 (24.0%) of 50 eyes.

• **IMAGING—FLUORESCEIN ANGIOGRAPHY AND INDOCYANINE GREEN ANGIOGRAPHY:** On FA, transmitted hyperfluorescence corresponded to areas of chorioretinal atrophy and blocked hypofluorescence corresponded to areas of dense pigmentation. These hypofluorescent areas were surrounded by hyperfluorescent zones. When comparing FA and FAF images, the extent of fundus abnormalities was more widespread on FAF images than on FA images (Figure 7).

The ICG demonstrated hypofluorescence along the retinal vessels in all phases. It revealed that hypofluorescence covered the chorioretinal atrophic lesions and partly extended into the areas that were grayish lesions on fundus photography and hyperfluorescent on FA. When comparing ICG and FAF images, the extent of hyperautofluorescence was more widespread on FAF images than on ICG images (Supplementary Figure S2). This indicates that choriocapillary atrophy is underestimated using FA, and evaluation may be improved with ICG. Moreover, ICG may underestimate the extent of affected lesions, and FAF is essential to evaluate the extent of lesions.

• **VISUAL FUNCTION—VISUAL FIELD AND VISUAL ACUITY:** Supplementary Table S2 demonstrates characteristics in visual field defects, changes in visual acuity, and

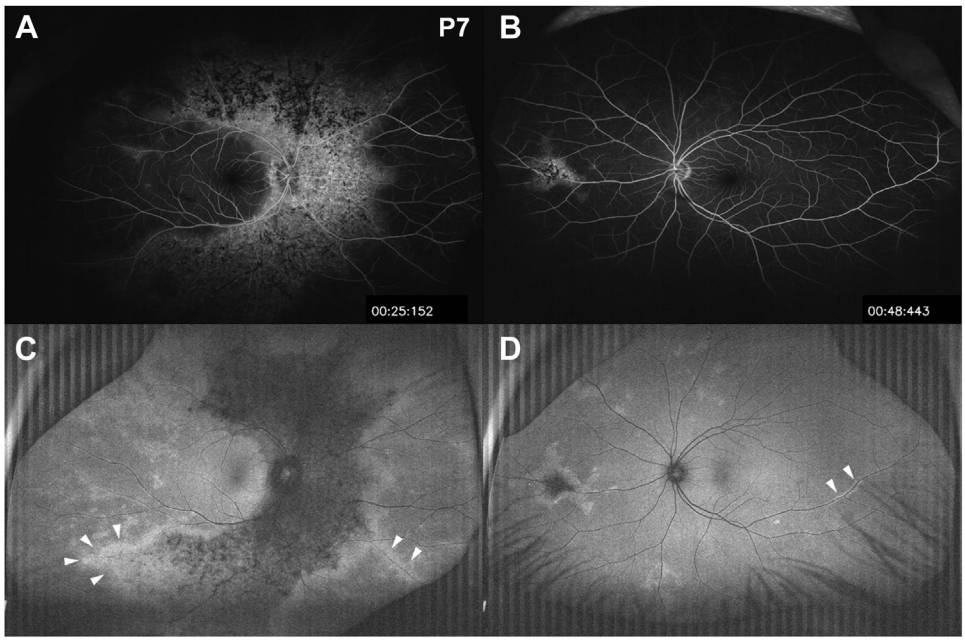

FIGURE 7. Ultrawide-field FA and FAF imaging of patient 7. (A, B) The FA images showing bilateral asymmetric speckled hyperfluorescence with blocked hypofluorescence within the affected lesions. (C, D) The fundus abnormalities were more widespread on FAF images than on FA images. The hyperautofluorescent lines appear at the edge of affected areas of hypoautofluorescent signal (white arrowheads). FA, fluorescein angiography, FAF = fundus autofluorescence, P = patient number.

electrophysiology findings. Visual field tests were available in 24 of 25 patients, with 1 (2.1%) of 48 eyes being normal. We observed 6 characteristics types of visual field defects: peripheral constriction (2 eyes, 4.2%), enlarged blind spot (6 eyes, 12.5%), geographic scotoma (27 eyes, 56.3%), central and temporal islands (4 eyes, 8.3%), central island (7 eyes, 14.6%), and peripheral islands (1 eye, 2.1%) (Supplementary Figure S3). In the "focal" type (8 eyes), 1 eye exhibited normal visual field, 4 eyes had enlarged blind spot, 2 eyes had peripheral constriction, and 1 eye had geographic scotoma. In the "paravenous" type (29 eyes), 2 eyes had enlarged blind spot, 21 eyes had geographic scotoma, 4 eyes had central island, and 2 eyes had central and temporal islands. In the "confluent" type (11 eyes), 5 eyes had geographic scotoma, 2 eyes had central and temporal islands, 3 eyes had central island, and 1 eye had peripheral islands. Therefore, in most participants, structural changes of chorioretinal atrophy with pigmentary disturbances in the retina were in concordance with functional changes in the visual field. However, there were several cases of discordance between structural and functional abnormalities.

Progression of visual field defects over time was also evaluated. Of the 24 patients who underwent visual field testing, 6 patients underwent only 1 examination and 36 eyes from 18 patients underwent at least 2 examinations. During the follow-up period, 20 eyes (55.6%) exhibited no definite progression in visual field defect at a mean of 5.05 ± 3.18 years (range, 0.54-9.26 years) and 16 eyes (44.4%) showed progression in visual field loss at a mean of 7.79 ± 3.32 years (range, 3.16-11.95 years). There were several cases of interocular asymmetry, which demonstrated that less severely affected eyes had relatively little change in visual field defect, but more severely affected eyes had progressed.

Visual acuities at the initial and final examination are shown in Figure 8, A and B. Thirty-nine eyes (78.0%) presented with an initial visual acuity of 20/50 (logMAR 0.4) or better and 36 eyes (72.0%) presented with a final visual acuity of 20/50 (logMAR 0.4) or better. Although the duration of the follow-up was variable, most patients did not experience significant changes in visual acuity during the follow-up period. Nevertheless, in some patients, severe deterioration in visual acuity was observed. Those who present with a significant decrease in vision were Patient 5 (both eyes), Patient 13 (right eye), Patient 6 (left eye), and Patient 19 (left eye). Patient 5 exhibited a symmetric paravenous type. The right eye of Patient 13 exhibited a paravenous type. The left eyes of Patient 6 and 19 exhibited a confluent type. All of these eyes demonstrated macular involvement.

• **ELECTROPHYSIOLOGIC EXAMINATIONS:** Electrophysiological assessment was available in 24 of 25 patients. Electrophysiological data were variable, ranging from normal and minor changes to markedly subnormal or completely extinguished ERG. The amplitude of the ERG response (% of lower limit of normal) has been rated as mild dysfunction (70%-99%), moderate dysfunction (30%-69%), severe dysfunction (<30%), and extinguished (indistinguishable

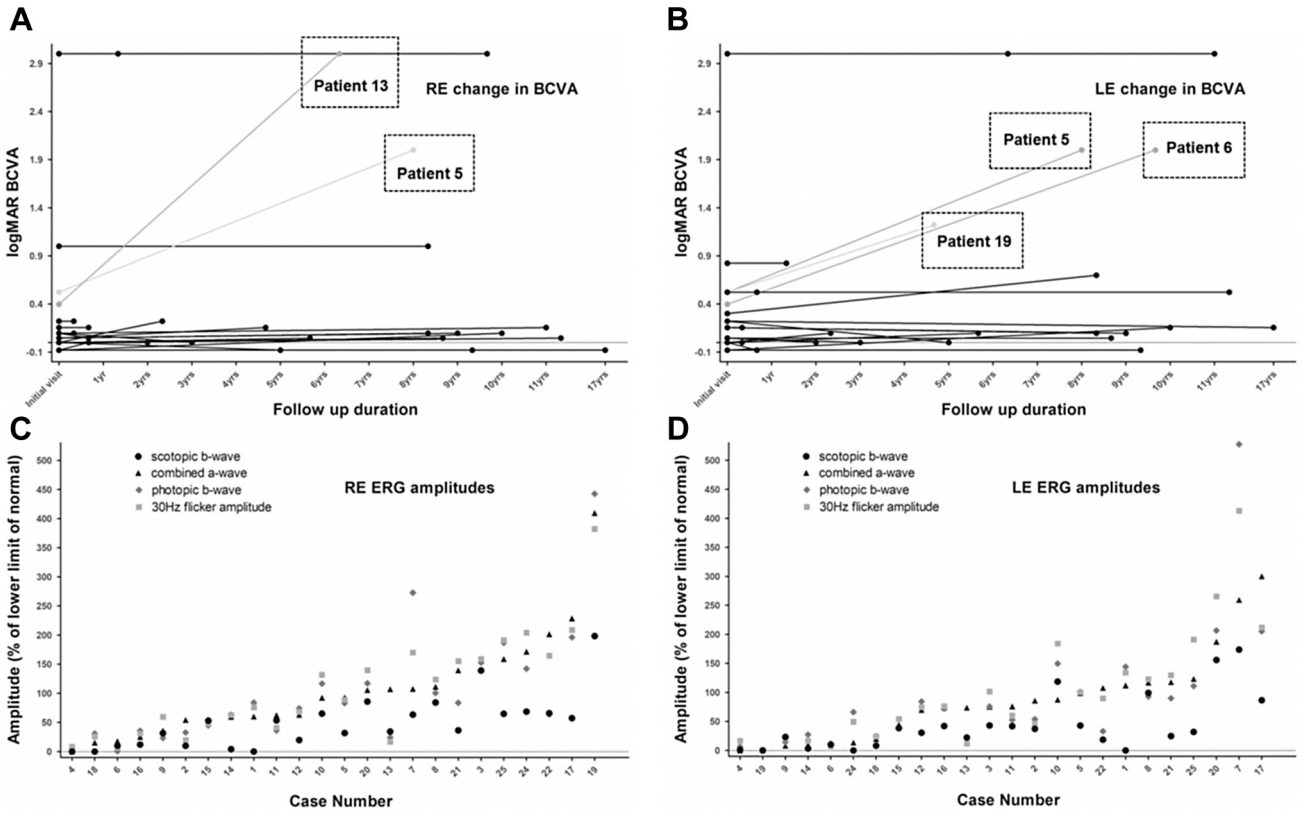

FIGURE 8. (A, B) Change in visual acuities at initial and final visits and (C, D) summary of full-field ERG parameters. Changes in best-corrected visual acuity (BCVA) in logMAR units of the (A) right and (B) left eyes show that most eyes retained a visual acuity of 20/50 (logMAR 0.4) or better during long-term follow-up. However, Patient 5, both eyes; Patient 13, right eye; Patient 6, left eye; and Patient 19, left eye, experienced a significant deterioration in vision. Summary of full-field ERG parameters in the (C) right and (D) left eyes demonstrate scotopic rod b-wave, maximum a-wave, photopic cone b-wave, and 30-Hz flicker amplitudes. Data are arranged according to the ascending order of maximum ERG a-wave amplitudes. ERG = electroretinography.

from zero). A generalized rod dysfunction with a relatively normal cone response was observed in 14 eyes (29.2%); this dysfunction was mild in 6 eyes, moderate in 5 eyes, and severe in 3 eyes. Greater rod than cone system involvement was found in 15 eyes (31.3%); this was moderate in 8 eyes and severe in 7 eyes. We noticed a similar degree of generalized rod and cone system dysfunction in 10 eyes (20.8%); this was mild in 3 eyes, moderate in 3 eyes, and severe in 4 eyes. The ERG was nearly totally extinguished in 5 eyes (10.4%) and normal in 4 eyes (8.3%). We found a high degree of interocular symmetry in all full-field ERGs in 13 (54.2%) of 24 patients. ERG data were asymmetric in 11 patients (45.8%). Figure 8, C and D, summarizes the corresponding full-field ERG amplitudes of the included patients.

Comparing the types of visual field defects and full-field ERG subtypes, out of the 6 eyes with enlarged blind spot, 3 eyes showed normal ERG findings and 3 eyes showed generalized rod dysfunction (mild in 1 eye and moderate in 2 eyes). Moreover, 2 eyes with peripheral constriction exhibited ERG findings of generalized rod dysfunction (severe), revealing that the cone function was relatively preserved in types of visual field defects of enlarged blind spot and peripheral constriction. Eyes with severe visual field loss such as central island, central and temporal islands, and peripheral islands demonstrated severe dysfunction in ERG findings as follows: generalized rod dysfunction (severe) in 1 eye, generalized rod and cone dysfunction (severe) in 2 eyes, generalized rod > cone dysfunction (severe) in 4 eyes, and totally extinguished in 5 eyes. Eyes with geographic scotoma exhibited varying degrees of ERG abnormalities depending on the extent of chorioretinal atrophy as follows: generalized rod > cone dysfunction (moderate in 8 eyes, severe in 3 eyes), generalized rod and cone dysfunction (mild in 3 eyes, moderate in 3 eyes, severe in 2 eyes), and generalized rod dysfunction (mild in 4 eyes, moderate in 2 eyes).

DISCUSSION

THIS STUDY AIMED TO INCREASE THE APPRECIATION AND recognition of PPCRA, a unique condition previously reported in only a limited number of case series.[3–6]

Although Shona and associates[20] have recently reported the clinical features of a similar number of PPCRA patients, the visual field data and diverse multimodal imaging were limited. The present study demonstrates the variable clinical spectrum and detailed analysis on multimodal imaging for a large cohort of 25 affected PPCRA patients seen at a single center.

The average age of the patients was 51.64 years ("middle age"), but the age of subjects ranged from 29 to 82 years. There was no sex predilection. Thirty-six percent of patients were asymptomatic and identified incidentally during routine medical examination. Contrary to what is generally believed, nyctalopia is not common in affected patients[21]; a considerable proportion (36.0%) of patients in our cohort complained of nyctalopia. There were no cases of families ascertained with PPCRA. Even though 2 patients revealed that their mother had poor night vision, they could not be confirmed by ophthalmologic evaluation. The average age of the patients in our study was higher than that in a previous study by Shona and associates[20] (36.6 years). This difference may be explained through the definitions of age in our studies. Our analysis was based on the patient's current age, while Shona and associates' analysis[20] was based on the age at initial presentation. The mean age at initial presentation of the current study was 45.28 years (range, 21-81 years). Because many asymptomatic patients were also included, disease onset age based on the onset of symptoms is difficult to figure out, but it is likely to be younger than this. Ethnic reasons or a selection bias in the tertiary hospital cohort could be attributed to the existing discrepancy in the mean age at initial presentation between the previous and the current study.

The typical funduscopic appearance of PPCRA is a bilaterally symmetrical accumulation of pigment and chorioretinal atrophy distributed along the retinal veins. However, not all patients had typical fundus findings, and the conditions appear to have variable expressivity. We identified chorioretinal atrophy as subretinal yellowish or grayish lesions that manifest as contiguous patches around the retinal vessels, coexisting with absent or depigmented retinal pigment epithelium that arborizes and spreads into the peripheral retina with the vasculature. The pigmentation varied in degree and appeared as typical bone corpuscle pigmentation, fine pigmentary changes, or coarse pigment clumps. Focal lesions mainly affected separate peripapillary and posterior pole regions. The chorioretinal atrophy region confined to a paravenous distribution, seen in the paravenous type, gradually merged in the more severe form of the confluent type, leaving the normal retina like an island and demonstrating a distinctly scalloped appearance.

Macular involvement has rarely been reported in PPCRA.[4,8,9,22–24] Visual acuity in PPCRA also has been reported to be generally unaffected or minimally decreased.[4,25] Macular changes demonstrated in previous studies include an epiretinal membrane, cystoid macular edema, lamellar macular hole, retinal pigment epithelial atrophy, and macular coloboma.[4,22–24] In our cohort, macular involvement was observed in 26.0% of patients and 5 of 13 eyes with macular involvement showed a significant decrease in visual acuity during the follow-up period. Therefore, although most PPCRA patients did not experience a significant reduction in vision, severe deterioration of vision has been observed in patients with macular involvement. Severely reduced vision has been reported as a result of rare changes, such as anisometropic amblyopia,[8] glaucoma,[26,27] nystagmus,[8,9] cataracts,[17] and vitreous opacity.[25] However, in the present study, macular involvement was the most common cause of the loss of vision, and other macular comorbidities, including epiretinal membrane and foveoschisis, had little effect on vision loss.

Although a bilateral symmetric appearance is known to be typical, the proportion of patients with a markedly asymmetric pattern in the current study was 40.0%. Certain reported cases have been markedly asymmetric or unilateral.[1,9,28,29] PPCRA has several clinical features similar to RP, and a few studies have suggested that PPCRA and RP phenotypes are part of the same spectrum of genetic disorders.[30,31] Traversi and associates[32] reported a case of unilateral RP with macular involvement in the mother and hereditary PPCRA in the daughter and son supporting this hypothesis. The observations from this report indicate that it was retinal pigment epithelium damage that is transmitted in an autosomal dominant manner with variable expression. An additional family case of siblings with PPCRA where the younger brother was more severely affected than his older sister provides additional support.[10] However, there is still no convincing evidence whether PPCRA is a genetic disorder and what its mode of transmission is, and the underlying basis of the disease remains controversial. Because the diagnosis of PPCRA is heavily based on typical and characteristic fundus appearance, the "confluent" type is likely to be mistaken for RP. If the genetic information of these patients was also investigated, it may be helpful for differential diagnosis from RP. At this time, it is difficult to suggest diagnostic criteria such as an inherited retinal disease panel negative. However, for the diagnosis of PPCRA, it would be necessary to exclude pseudo-PPCRA disease along with the previously suggested diagnostic criteria. Differential diagnoses include chorioretinal degeneration and inflammatory diseases that cause chorioretinal atrophy, including pericentral, sectoral, and typical RP, serpiginous choroidopathy, helicoid peripapillary chorioretinal atrophy, hydroxychloroquine retinopathy, and autoimmune retinopathy.

Contrary to previous reports that the main region affected in PPCRA is the retinal pigment epithelium,[17,33,34] Barteselli[35] demonstrated that choroidal thinning precedes development of frank retinal pigment epithelial atrophy. It was hypothesized that decreased blood flow secondary to choroidal thinning may lead to

insufficient metabolic supplementation for the outer retinal structures, leading to thinning and atrophy of the photoreceptor first and of the retinal pigment epithelium later in the disease.[35] Previous reports have also suggested the relationship between choriocapillaris hypoperfusion and the development of PPCRA.[36,37] In the current study, patients in whom the retinal pigment epithelium was unaffected were often associated with visible thinning of the underlying choroid. Therefore, we assume that choroidopathy may precede retinal pigment epithelial abnormalities, however, the mechanisms for the development of PPCRA must be further investigated.

Multimodal imaging is not necessarily essential for the diagnosis of PPCRA, but it is a useful tool for the assessment of this unique population. Ultrawide-field imaging captures up to 200 degrees of the retina in a single click without much patient cooperation. PPCRA is likely to be misdiagnosed as RP using conventional fundus photography. The typical appearance of PPCRA lesions along the retinal veins extending from the disc to the periphery is preferentially seen in ultrawide-field imaging. The exact extent of chorioretinal atrophy was often more and better delineated on FAF imaging than on color or FA images. The transition zone with sharp demarcation lines between viable and affected areas has been previously reported.[38] The retinal pigment epithelial cells in the transition zone bear an increased metabolic burden and have an excess accumulation of lipofuscin. This is the reason that hyperautofluorescent lines appear at the edge of affected areas. When the photoreceptors are damaged, the metabolic demand of retinal pigment epithelium is reduced. Following the final retinal pigment epithelial atrophy, these areas eventually become hypoautofluorescent. The FA and ICG are useful for differentiating PPCRA from retinal vasculitis with infectious or inflammatory causes, and OCT is essential for evaluating the microstructures of the fovea and macular involvement. Therefore, multimodal imaging enables accurate diagnosis of disease, categorizes and provides understanding to various types of disease, and is useful for the follow-up of these cases and predicting visual prognosis.

In previous reports, visual field findings have ranged from normal to severe constriction.[25,39] Depending on the topography of the chorioretinal atrophy and pigmentation, the visual field may manifest as a ring scotoma,[9] geographic scotoma,[4] paracentral scotomas,[9,27,40] concentric constriction,[1,24,27,40] an enlarged blind spot,[15,17] or scattered scotomas.[39] In the current study, there were patients with visual field abnormalities that did not match with the fundus appearance. We speculate on the possible reasons for discordance between structural changes of chorioretinal atrophy with pigmentary disturbances in the retina and functional changes in the visual field. First, the classification of the PPCRA phenotype according to the fundus appearance is inherently arbitrary. Indeed, there are cases in which paravenous and confluent patterns are mixed in one eye of the patient. A more delicate classification system that can reflect the severity of functional changes in the disease might be necessary. Second, it is possible that the retinal area where the pigmentary disturbance that is not apparent is also not necessarily normal. Accordingly, even if the fundus appears less severe than it actually is, more severe visual field abnormalities may be observed. Shona and associates[20] reported that no progression of visual field loss was found in 7 cases. However, in our cohort, 44.4% of eyes exhibited a definite progression in visual field loss during long-term follow-up. In particular, eyes with confluent type showed severe visual field loss, such as central and temporal islands, a central island, or a peripheral island.

A wide range of ERG abnormalities has been reported in PPCRA, from normal to totally extinguished responses.[18] B-wave amplitude reduction is the most common observation, followed by A-wave amplitude reduction and delayed latency.[7,15,25,41] In specific cases, ERGs have revealed a decreased scotopic response with a normal photopic response and vice versa in other patients.[8,15] In our cohort, however, rod dysfunction was often more severe than cone dysfunction, and significant interocular ERG asymmetry was common. It was hypothesized that scotopic responses reflect the size and extent of atrophic lesions, whereas the bright flash and photopic responses apparently did not parallel changes in lesion size.[18]

There are several limitations to this study. First, this study was retrospective and a selection bias could have accentuated some estimates and masked others. Second, not performing genetic analyses of the patient cohort and examination of other family members to demonstrate more evidence regarding the underlying basis of the disease is a limitation of our study. Third, the study included a small number of patients with variable follow-up period. However, because PPCRA is very rare, our case series is the largest as of this writing to our knowledge. We believe that the current study has several strengths, such as that it included the largest number of patients and the analysis of high-quality multimodal imaging, and visual field and electrophysiological assessments were included.

In conclusion, PPCRA is a rare disorder that is not well understood. In our patients, contrary to what is generally believed, nyctalopia was common (36.0%). The proportion of eyes with macular involvement was quite high (26.0%), and the visual prognosis was poor in these patients. We show that interocular asymmetry was common not only regarding structural aspects such as fundus appearance (40.0%), but also in functional aspects such as ERG (45.8%). Most patients exhibited no apparent changes in fundus appearance and retained stable vision over time. Nevertheless, when OCT changes were included, the proportion of eyes with structural progression was 24.0% and the proportion of eyes with functional progression in the visual field was 44.4%. Multimodal imaging can provide insights into the clinical characteristics of this disorder to facilitate diagnosis and classification and follow-up of these patients.

CRediT AUTHORSHIP CONTRIBUTION STATEMENT

EUN KYOUNG LEE: CONCEPTUALIZATION, METHODOLOGY, Formal analysis, Writing - original draft. **Sang-Yoon Lee:** Formal analysis, Writing - review & editing. **Baek-Lok Oh:** Data curation, Formal analysis. **Chang Ki Yoon:** Data curation, Formal analysis. **Un Chul Park:** Data curation, Formal analysis. **Hyeong Gon Yu:** Investigation, Resources, Supervision.

FUNDING/SUPPORT: THIS STUDY WAS SUPPORTED BY A RESEARCH GRANT OF THE SEOUL NATIONAL UNIVERSITY HOSPITAL (0620200030), funded by the Korean Association of Retinal Degeneration (KARD-2019001) and was also supported in part by a grant of the Korea Health Technology R&D Project through the Korea Health Industry Development Institute (KHIDI), funded by the Ministry of Health & Welfare, Republic of Korea (grant number: HI14C1277). KARD had no role in the design or conduct of this research. The Biospecimens and data used in this study were provided by the Biobank of Seoul National University Hospital, a member of Korea Biobank Network. Financial Disclosures: The authors indicate no financial support or conflicts of interest. All authors attest that they meet the current ICMJE criteria for authorship.

REFERENCES

1. Limaye SR, Mahmood MA. Retinal microangiopathy in pigmented paravenous chorioretinal atrophy. *Br J Ophthalmol* 1987;71(10):757–761.
2. Brown TH. Retino-choroiditis radiata. *Br J Ophthalmol* 1937; 21(12):645–648.
3. Noble KG, Carr RE. Pigmented paravenous chorioretinal atrophy. *Am J Ophthalmol* 1983;96(3):338–344.
4. Johansen J, Lund-Andersen C, Autzen T. Pigmented paravenous chorioretinal atrophy. *Acta Ophthalmol (Copenh)* 1988; 66(4):474–477.
5. Kukner AS, Yilmaz T, Celebi S, Aydemir O, Ulas F. Pigmented paravenous retinochoroidal atrophy. A literature review supported by seven cases. *Ophthalmologica* 2003; 217(6):436–440.
6. Choi JY, Sandberg MA, Berson EL. Natural course of ocular function in pigmented paravenous retinochoroidal atrophy. *Am J Ophthalmol* 2006;141(4):763–765.
7. Skalka HW. Hereditary pigmented paravenous retinochoroidal atrophy. *Am J Ophthalmol* 1979;87(3):286–291.
8. Traboulsi EI, Maumenee IH. Hereditary pigmented paravenous chorioretinal atrophy. *Arch Ophthalmol* 1986;104(11): 1636–1640.
9. Noble KG. Hereditary pigmented paravenous chorioretinal atrophy. *Am J Ophthalmol* 1989;108(4):365–369.
10. Obata R, Yanagi Y, Iriyama A, Tamaki Y. A familial case of pigmented paravenous retinochoroidal atrophy with asymmetrical fundus manifestations. *Graefes Arch Clin Exp Ophthalmol* 2006;244(7):874–877.
11. McKay GJ, Clarke S, Davis JA, Simpson DA, Silvestri G. Pigmented paravenous chorioretinal atrophy is associated with a mutation within the crumbs homolog 1 (CRB1) gene. *Invest Ophthalmol Vis Sci* 2005;46(1):322–328.
12. Small KW, Anderson WB Jr. Pigmented paravenous retinochoroidal atrophy. Discordant expression in monozygotic twins. *Arch Ophthalmol* 1991;109(10):1408–1410.
13. Kellner U, Helbig H, Foerster MH. [Phenocopies of hereditary retinal degenerations]. *Ophthalmologe* 1996;93(6): 680–687 [in German].
14. Peduzzi M, Guerrieri F, Torlai F, Prampolini ML. Bilateral pigmented paravenous retino-choroidal degeneration following measles. *Int Ophthalmol* 1984;7(1):11–14.
15. Foxman SG, Heckenlively JR, Sinclair SH. Rubeola retinopathy and pigmented paravenous retinochoroidal atrophy. *Am J Ophthalmol* 1985;99(5):605–606.
16. Chi HH. Retinochoroiditis radiata. *Am J Ophthalmol* 1948; 31(11):1485–1487.
17. Yamaguchi K, Hara S, Tanifuji Y, Tamai M. Inflammatory pigmented paravenous retinochoroidal atrophy. *Br J Ophthalmol* 1989;73(6):463–467.
18. Huang HB, Zhang YX. Pigmented paravenous retinochoroidal atrophy (Review). *Exp Ther Med* 2014;7(6):1439–1445.
19. Constable PA, Bach M, Frishman LJ, Jeffrey BG, Robson AG. ISCEV Standard for clinical electro-oculography (2017 update). *Doc Ophthalmol* 2017;134(1):1–9.
20. Shona OA, Islam F, Robson AG, et al. Pigmented paravenous chorioretinal atrophy: detailed clinical study of a large cohort. *Retina* 2019;39(3):514–529.
21. Brooks DN, Potter JW, Bartlett JD, Nowakowski R. Pigmented paravenous retinochoroidal atrophy. *J Am Optom Assoc* 1980;51(12):1097–1101.
22. Romero R, Castano A, Moriche M, Poyales B, Granados M. Pigmented paravenous retinochoroidal atrophy with macular involvement. *Arch Soc Esp Oftalmol* 2013;88(2):77–79.
23. Ahmed AS, Rishi P. A rare presentation of pigmented paravenous retinochoroidal atrophy. *Oman J Ophthalmol* 2015; 8(1):47–49.
24. Chen MS, Yang CH, Huang JS. Bilateral macular coloboma and pigmented paravenous retinochoroidal atrophy. *Br J Ophthalmol* 1992;76(4):250–251.
25. Batioglu F, Atmaca LS, Atilla H, Arslanpence A. Inflammatory pigmented paravenous retinochoroidal atrophy. *Eye (Lond)* 2002;16(1):81–84.
26. Bozkurt N, Bavbek T, Kazokoglu H. Hereditary pigmented paravenous chorioretinal atrophy. *Ophthalmic Genet* 1998; 19(2):99–104.
27. Al-Husainy S, Sarodia U, Deane JS. Pigmented paravenous retinochoroidal atrophy: evidence of progression to macular involvement in a family with a 42-year history. *Eye (Lond)* 2001;15(Pt 3):329–330.
28. Cheung DS. Pigmented paravenous chorioretinal atrophy. *Am J Ophthalmol* 1984;97(1):113.
29. Charbel Issa P, Scholl HP, Helb HM, et al. [Unilateral pigmented paravenous retinochoroidal atrophy]. *Klin Monbl Augenheilkd* 2007;224(10):791–793.
30. Ratra D, Chandrasekharan DP, Aruldas P, Ratra V. Concurrent retinitis pigmentosa and pigmented paravenous retinochoroidal atrophy phenotypes in the same patient. *Indian J Ophthalmol* 2016;64(10):775–777.
31. Aoki S, Inoue T, Kusakabe M, et al. Unilateral pigmented paravenous retinochoroidal atrophy with retinitis pigmentosa

in the contralateral eye: A case report. *Am J Ophthalmol Case Rep* 2017;8:14–17.
32. Traversi C, Tosi GM, Caporossi A. Unilateral retinitis pigmentosa in a woman and pigmented paravenous chorioretinal atrophy in her daughter and son. *Eye (Lond)* 2000;14(Pt 3A):395–397.
33. Yamaguchi K, Kin-para Y, Tamai M. Idiopathic central serous choroidopathy in a patient with pericentral pigmentary retinal degeneration. *Ann Ophthalmol* 1991;23(7):251–253.
34. Young WO, Small KW. Pigmented paravenous retinochoroidal atrophy (PPRCA) with optic disc drusen. *Ophthalmic Paediatr Genet* 1993;14(1):23–27.
35. Barteselli G. Fundus autofluorescence and optical coherence tomography findings in pigmented paravenous retinochoroidal atrophy. *Can J Ophthalmol* 2014;49(6):e144–e146.
36. Cicinelli MV, Giuffre C, Rabiolo A, Parodi MB, Bandello F. Optical coherence tomography angiography of pigmented paravenous retinochoroidal atrophy. *Ophthalmic Surg Lasers Imaging Retina* 2018;49(5):381–383.
37. Shen Y, Xu X, Cao H. Pigmented paravenous retinochoroidal atrophy: a case report. *BMC Ophthalmol* 2018;18(1):136.
38. Takagi S, Hirami Y, Takahashi M, et al. Use of wide-field fundus camera, fundus autofluorescence, and OCT in cases of pigmented paravenous retinochoroidal atrophy. *Ophthalmol Retina* 2018;2(1):79–81.
39. Parafita M, Diaz A, Torrijos IG, Gomez-Ulla F. Pigmented paravenous retinochoroidal atrophy. *Optom Vis Sci* 1993; 70(1):75–78.
40. Yanagi Y, Okajima O, Mori M. Indocyanine green angiography in pigmented paravenous retinochoroidal atrophy. *Acta Ophthalmol Scand* 2003;81(1):60–67.
41. Hirose T, Miyake Y. Pigmentary paravenous chorioretinal degeneration: fundus appearance and retinal functions. *Ann Ophthalmol* 1979;11(5):709–718.